Strong-Field Induced Vibrational Coherence in the Ground Electronic State of Hot I_2

L. Fang and G. N. Gibson

Department of Physics, University of Connecticut, Storrs, Connecticut 06269, USA

(Received 8 July 2007; published 13 March 2008)

We observe large amplitude coherent vibrations in vibrationally hot ground state neutral I_2 molecules created through "Lochfrass," or "*R*-selective ionization." We directly measure the phase and amplitude of the vibrations. Our results support the notion of enhanced ionization at large internuclear separation over recent theoretical predictions for heavy molecules. Furthermore, simulations of the vibrational motion show that for Lochfrass the vibrational coherence, contrary to most coherent control schemes, is stronger for hot molecules than for cold molecules.

DOI: 10.1103/PhysRevLett.100.103003 PACS numbers: 33.80.Rv, 32.80.Rm, 42.50.Hz

For decades, vibrational coherence has played a crucial role in the studies of molecular structure, molecular interactions with electric fields, molecular dynamics, and quantum dynamic control [1–4]. The creation of vibrational wave packets (VWPs) in excited electronic molecular states with laser pulses can be achieved through resonant multiphoton excitation or multiphoton ionization [3,5–8]. While VWPs in the ground electronic state (GES) of neutral molecules have been produced with resonant interactions [5–7], two nonresonant methods have recently been proposed: bond softening (BS), a time-dependent description of off-resonant two-photon Raman scattering, and "Lochfrass" ("hole-eating") [9,10]. Moreover, in the available experiments regarding all schemes, to the authors' best knowledge, (1) the molecules were initially cold [5–8], that is only the $\nu = 0$ vibrational level was populated, and coherent population in higher levels was created through the interaction with the laser field; (2) the vibrations were detected only through variations in total ionization rates, rather than a measurement that directly yields the spatial structure of the VWP.

In this Letter, we present studies of VWPs created by short laser pulses in the GES of room-temperature I_2 for which the $\nu = 0$ vibrational state contains only 59% of the initial population and up to 5 vibrational levels have significant population [11]. To probe the VWP, we use a second pulse to ionize it to a highly dispersive state of I_2^{2+} (see Fig. 1) that dissociates into $I^{2+} + I^{0+}$ [we denote this state as (2,0)] [12], and measure both the variation in population of the probing state as addressed in earlier work, and the variation in kinetic energy release (KER). This allows us to directly map the motion of the VWP in the GES as a function of internuclear separation R and obtain the phase of the vibrations.

We conclude that Lochfrass is the dominant mechanism exciting the VWPs given our experimental conditions and results rather than BS. We will discuss how these can be distinguished below. Lochfrass has recently been demonstrated by experiments concerning the generation of GES VWPs in D_2 molecules [9], in which cold D_2 was used and variations of the population in states of D_2^+ were observed. This scheme is outlined in Fig. 1: a short laser pulse (pump pulse) partially ionizes all the initially populated vibrational states of the GES with an R-dependent ionization rate $\Gamma(R)$. The wave functions are deformed in such a way that the remaining wave functions are partially coherent and lead to a wave packet (WP) in the GES. Depleted asymmetrically with respect to the equilibrium position, the WP starts its vibrational motion in the direction that the wave functions were depleted. In this way, the laser ionizes a spatial hole in the wave function, which then starts to evolve. This is similar to dark WPs in Rydberg states which are also created through R-dependent ionization [13].

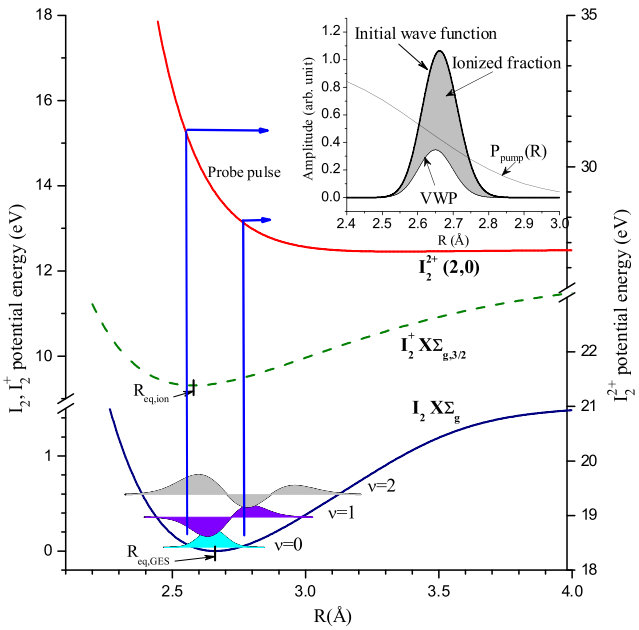

FIG. 1 (color online). Schematic potential energy curves [12,16,23], showing the physical scenario of the experiments. Only wave functions of the first three vibrational states after ionization by the pump pulse are shown [31]. Inset: $\nu = 0$ eigenfunction and wave function after it is partially ionized with an R-dependent ionization rate. $P_{\text{pump}}(R)$ is the survival probability in the GES after ionization by the pump pulse.

In addition to the experiments, we also simulate the preparation of the VWPs with the Lochfrass scheme. The simulations are consistent with our data, showing the validity of the generation scheme and allow us to explore the temperature dependence of the VWPs. Remarkably, we find that the VWPs in the GES are stronger in hot molecules compared with cold molecules. This stronger coherence with higher temperature runs counter to all coherent control schemes that we are aware of.

The experimental setup has been described in our previous work [12,14,15]. In brief, the laser system is a standard Ti:sapphire laser system consisting of a short-pulse oscillator and a multipass amplifier. The pump and probe laser pulses are created with a Michelson interferometer. The final pulses are 23 fs, transform limited, centered at 790 nm, linearly polarized, and generated at a 1 kHz repetition rate, with energies of each pulse up to several tens of μJ. The laser beam is focused to a $\sim$25-μm diameter spot producing an intensity on the order of 10^{13} W/cm^2. Room-temperature (295 K) I_2 molecules are leaked effusively into a standard high vacuum chamber with a base pressure of 1×10^{-9} torr. Tests were performed to ensure space charge was not affecting the KER of the ions. The ion signals are detected with a pair of microchannel plates in a standard time-of-flight (TOF) spectrometer. The time when the two pulses overlap (t_0) is determined by the enhanced ion signal in the bound I_2^{3+} channel at t_0 with an uncertainty of 10 fs.

Figure 2(a) shows the KER spectrum of the (2,0) channel converted from the TOF spectrum as a function of pump-probe delay (τ). Integrating the data in Fig. 2(a) over a range of KER that covers only the (2,0) channel, we obtain the variation of the signal as a function of τ, $S(\tau)$, as shown in Fig. 2(b). The variation in the population is found to have a large contrast of $\sim$30%, also shown in Fig. 3(a). Fitting the signal with $S(\tau) = S_0 + \Delta S \times \cos((2\pi/T_p)\tau - \varphi_s)$ over 40 cycles yields a vibrational period of $T_p = 158 \pm 2$ fs and a phase of $\varphi_s = 0.64\pi$. S_0 and ΔS are the average and modulated signals, respectively. According to the measured vibrational period, we determine that the VWP is created in the GES of I_2, which has a vibrational period of 155 fs for the $\nu = 0$ state [16]. The measured value is slightly higher, because, for room-temperature I_2, higher vibrational levels associated with longer vibrational periods are initially populated and participate in the VWP. Moreover, our simulations of room-temperature I_2 molecules yield a vibrational period consistent with the data. Finally, no other easily accessible state of I_2 or I_2^+ has this vibrational period [16–21].

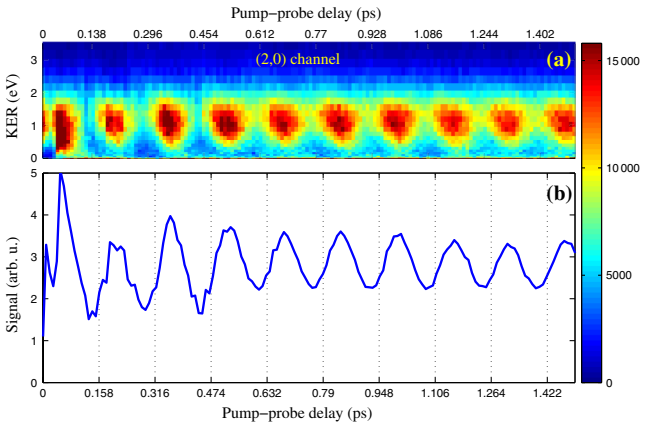

FIG. 2 (color online). (a) KER data of the (2,0) channel as a function of τ. (b) Variation of signal in the (2,0) channel as a function of τ. Data were taken with a pump-probe intensity ratio of 1:2, where the pump pulse intensity is estimated to be $\sim 4.6 \times 10^{13}$ W/cm^2. The I_2 pressure is $\sim 6 \times 10^{-6}$ torr.

We also find a modulation in the peak KER from the data in Fig. 2(a) by fitting the KER spectrum for each τ with a Gaussian function. Figure 3(b) shows the peak KER as a function of τ, KER(τ). Using the potential energy curve of the (2,0) state [12], we project KER(τ) to $R(\tau)$, as shown in Fig. 4 (dots). As above, we define a phase through $R(\tau) = R_{\text{ave}} + \Delta R \cos((2\pi/T_p)\tau - \varphi_R)$, where R_{ave} is the average R at $T = 295$ K and ΔR is the modulation of R. We find that the vibrational amplitude $2\Delta R = 0.035$ Å and $\varphi_R = 0.81\pi$. The phase corresponds to the WP being created at the inner turning point (TP) to within 15 fs of t_0, which is less than the pulse duration.

The phase of the WP motion has been used to distinguish between Lochfrass and BS as the mechanism producing the vibrational motion [9]. For Lochfrass, if the ionization rate increases (decreases) as a function of R, then the initial wave function will be depleted more at large (small) R and the expectation value of R ($\langle R \rangle$) for the newly created WP

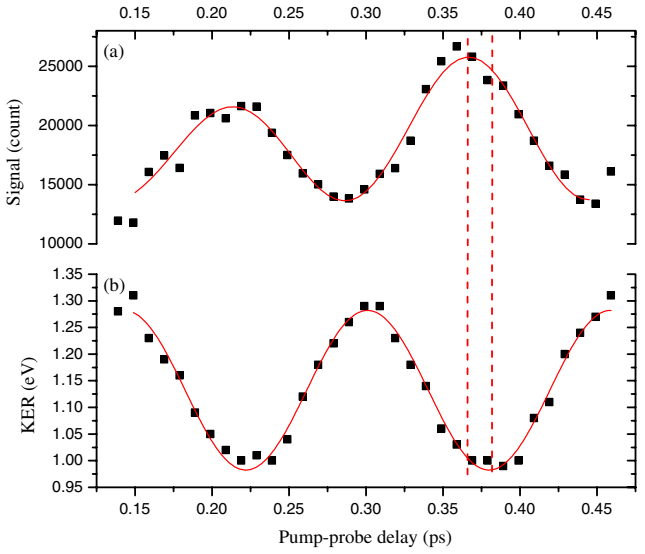

FIG. 3 (color online). (a) Ion signal in the (2,0) channel as a function of τ. (b) Peak values of the KER spectra for the (2,0) channel as a function of τ, from data shown in Fig. 2. Solid lines: fittings of data with a cos function and a slowly varying envelope. Dashed lines mark the extreme positions of the cos function near $\tau = 0.375$ ps indicating a phase shift.

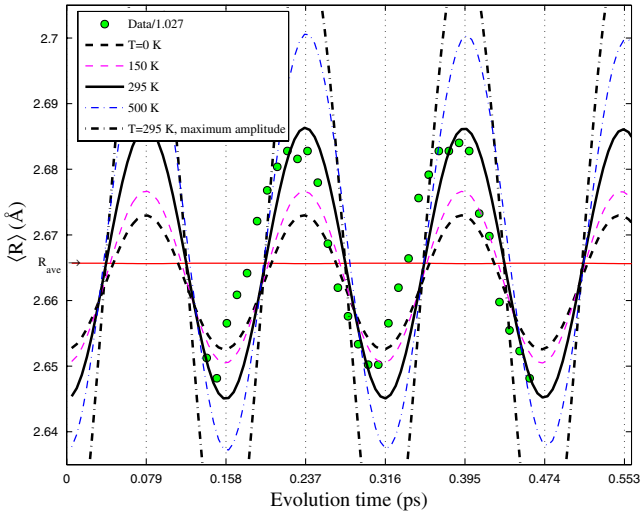

FIG. 4 (color online). Measured values of the expectation value of R of the VWP along with simulations in the GES at different initial temperatures. All simulations use a survival probability $P_{\text{pump}}(R)$ with $r_{\text{erf}} = 2.62$ Å and $\beta_{\text{erf}} = 0.31$ Å (see text). The curve labeled "maximum amplitude" is a separate simulation where there is no laser pulse and all phases are set to zero (see text). The data points are extracted from data shown in Fig. 2(a), and are scaled down by a factor of 1.027, which is within the absolute uncertainty of our measurement of R, to match R_{ave} at $T = 295$ K, given by the straight line.

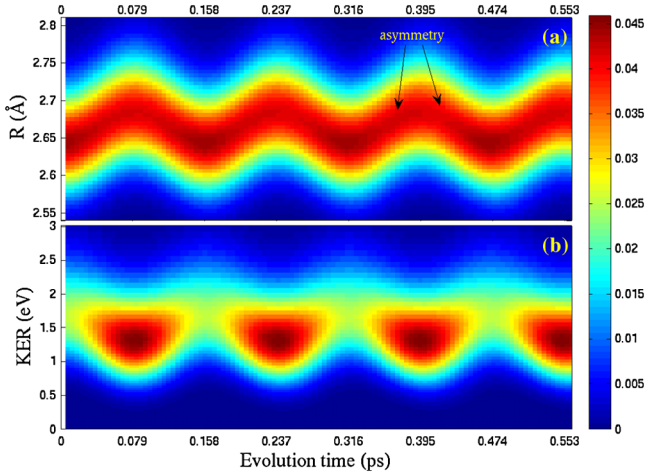

FIG. 5 (color online). (a) Simulation of the population of the VWP in the GES of room-temperature I_2 as a function of R and τ. The survival probability for the pump is the same as that in Fig. 4. (b) Simulation of the KER of the population ending up in the (2,0) channel after the probe. The simulation uses a ionization probability for the probe with $r_{\text{erf}} = 2.70$ Å and $\beta_{\text{erf}} = 0.15$ Å (see text).

will be a minimum (maximum) at t_0. In terms of the phase defined above, $\varphi_R = \pi$ ($\varphi_R = 0$). In the case of BS, the initial wave function will be released towards larger R during the rising edge of the pulse, as the bond softens, and will be pushed back to smaller R on the falling edge, as the bond hardens resulting in a phase of $\pi/2$, as determined in Ref. [9]. While the ion signal $S(t)$ can indirectly give $R(t)$ through modeling [9], we measure directly $R(t)$. From our measured value of the phase mentioned above, we conclude that Lochfrass is the dominant mechanism producing our observed vibrational motion and that the ionization rate increases for increasing R. However, the fact that the phase is less than π suggests that BS may also play a role. Only detailed molecular calculations can determine the exact extent.

Interestingly, having independently measured the ion signal $S(\tau)$ and position $R(\tau)$, we found that $S(\tau)$ is not exactly in phase with $R(\tau)$ (see Fig. 3), but leads $R(\tau)$ by 0.17π. This relative phase is not affected by the uncertainty of t_0 determination. This phase shift implies an asymmetry of the quantum evolution between the outgoing and ingoing WP [12], as shown in Fig. 5(a). Also, simulations show a nonzero phase shift of $\sim 0.03\pi$, although this depends on the exact form of $\Gamma(R)$. Thus, this phase shift provides a sensitive test of any modeling.

To further explore the coherent vibrations induced in hot molecules by intense-field ionization, we simulate the generation and evolution of the VWP in the GES as follows: the first 10 vibrational states are populated initially according to a Boltzmann distribution with random phases. Since we do not focus on the exact ionization rate as a function of R by the laser pulses, we simply model the survival probability in the GES after ionization by the pump pulse, with a modified error function $P_{\text{pump}}(R) = [1 - \text{erf}((R - r_{\text{erf}})/\beta_{\text{erf}})]/2$. The parameters are chosen for the best match of the simulations with the data in vibrational amplitude and asymmetry of the VWP (see caption of Fig. 4 for values of the parameters). We solve the time-dependent Schrödinger equation for the VWP after ionization [12]. Figure 5(a) shows the simulation result for the VWP's evolution as a function of time. A vibrational period of 158 fs is obtained, in good agreement with the data as mentioned above. Furthermore, we simulate the ionization of the VWP in Fig. 5(a) to the (2,0) state by the probe pulse with an ionization probability $I_{\text{probe}}(R) = [1 + \text{erf}((R - r_{\text{erf}})/\beta_{\text{erf}})]/2$ (see caption of Fig. 5 for values of the parameters). As shown in Fig. 5(b), the phase of the population in the (2,0) channel after the probe pulse indicates a start with small population as expected, and the VWP is shaped unevenly due to the R-dependent probe ionization. This results in a triangular shape for each patch and closely resembles our data shown in Fig. 2(a).

Since the simulations for room-temperature I_2 interpret the data well, we next use the simulations to predict the temperature dependence of the coherent vibrations. Figure 4 shows the vibrational amplitudes for different temperatures. The amplitude increases as the temperature of the ensembles increases or as more vibrational levels are initially populated. We also show two extreme situations where no laser is involved. The first corresponds to a thermal, or completely incoherent, ensemble of molecules,

which, of course, will show no change in R, indicated by R_{ave}. The second corresponds to the maximum possible vibrational motion obtained by setting all the phases of the vibrational eigenstates populated at room temperature to zero, i.e., perfect coherence of the vibrational states. The amplitude for vibrations excited by ionization in hot molecules is in between these two extremes and, therefore, demonstrates that the R-dependent ionization imposes certain phase relationships among the remaining wave functions to form a VWP.

Thus, a thermally hot ensemble is not necessarily detrimental to creating coherent states, at least for some types of interactions. The key, here, is the dissipative nature of the Lochfrass pulse. Since it selectively ionizes the wave functions, it can reduce the phase space of the thermal distribution. Thus, there are two routes to creating coherent motion starting from a pure ground state. First, a laser pulse can coherently populate upper states with the correct phases and amplitudes to produce the desired motion. This is the standard approach to coherent control. Alternatively, we demonstrate that the original excitation can be produced by heat, populating an incoherent superposition of states, and then a laser pulse can be used to reduce the phase space to that corresponding to the desired motion through a dissipative interaction.

As mentioned previously, according to the phase of $R(\tau)$, we conclude that, at R_e, $\Gamma(R)$ for the pump pulse increases as R increases. However, there is some disagreement in theoretical predictions on this point. On the one hand, $\Gamma(R)$ may be dominated by the ionization potential $I_p(R)$ of the molecule according to the standard Ammosov-Delone-Krainov (ADK) model [22]. For I_2, $I_p(R)$ has a minimum at an R less than R_e [16,23], and hence, at R_e $\Gamma(R)$ would be a decreasing function of R [24], opposite to what we observe. On the other hand, one of the most consistent features of strong-field ionization of molecules has been R-dependent enhanced ionization (REI) due to molecular structure which is not included in the standard ADK model. A critical internuclear separation R_c where $\Gamma(R)$ reaches a maximum, has been both theoretically predicted [25–27] and experimentally verified [28–30]. For diatomic molecules, R_c results from the dynamics of the double-well potential, occurs in both one- and two-electron molecules [25–27], and is found, so far, to be larger than R_e whether or not $I_p(R)$ has a minimum at that point [26]. Thus, REI predicts that $\Gamma(R)$ is increasing at R_e, as we observe from Lochfrass, suggesting that REI dominates the ionization rate in I_2.

In conclusion, we observe large amplitude coherent vibrational motion in the GES of room temperature I_2. The measured sign of the slope of the R-dependent ionization rate indicates REI in neutral I_2. Simulations show that R-dependent ionization by an intense laser pulse can induce stronger vibrational coherence in hot molecules than in cold, suggesting that hot ensembles of molecules are not necessarily detrimental to coherent control.

We would like to acknowledge support from the NSF under Grants No. PHYS-0244658 and No. PHYS-0653029.

[1] A. H. Zewail, J. Phys. Chem. **97**, 12 427 (1993).
[2] J. Itatani *et al.*, Phys. Rev. Lett. **94**, 123902 (2005).
[3] Th. Ergler *et al.*, Phys. Rev. Lett. **97**, 193001 (2006).
[4] Kevin F. Lee *et al.*, Phys. Rev. Lett. **93**, 233601 (2004).
[5] H. Schwoerer, R. Pausch, M. Heid, and W. Kiefer, Chem. Phys. Lett. **285**, 240 (1998).
[6] T. Baumert, V. Engel, C. Meier, and G. Gerber, Chem. Phys. Lett. **200**, 488 (1992).
[7] C. C. Hayden and D. W. Chandler, J. Chem. Phys. **103**, 10 465 (1995).
[8] T. Baumert *et al.*, J. Phys. Chem. **95**, 8103 (1991).
[9] Th. Ergler *et al.*, Phys. Rev. Lett. **97**, 103004 (2006).
[10] E. Goll, G. Wunner, and A. Saenz, Phys. Rev. Lett. **97**, 103003 (2006).
[11] We refer to molecules with $\nu > 0$ vibrational states initially populated as hot molecules.
[12] L. Fang and G. N. Gibson, Phys. Rev. A **75**, 063410 (2007).
[13] R. R. Jones and L. D. Noordam, Adv. At. Mol. Opt. Phys. **38**, 1 (1997).
[14] G. N. Gibson, R. N. Coffee, and L. Fang, Phys. Rev. A **73**, 023418 (2006).
[15] M. Li and G. N. Gibson, J. Opt. Soc. Am. B **15**, 2404 (1998).
[16] W. A. de Jong, L. Visscher, and W. C. Nieuwpoort, J. Chem. Phys. **107**, 9046 (1997).
[17] Q. Li and K. Balasubramanian, J. Mol. Spectrosc. **138**, 162 (1989).
[18] F. Martin, R. Bacis, S. Churassy, and J. Vergès, J. Mol. Spectrosc. **116**, 71 (1986).
[19] T. Ishiwata, H. Ohtoshi, M. Sakaki, and I. Tanaka, J. Chem. Phys. **80**, 1411 (1984).
[20] Andrew J. Yencha *et al.*, Chem. Phys. Lett. **229**, 347 (1994).
[21] M. C. R. Cockett, R. J. Donovan, and K. P. Lawley, J. Chem. Phys. **105**, 3347 (1996).
[22] M. V. Ammosov, N. B. Delone, and V. P. Krainov, Sov. Phys. JETP **64**, 1191 (1986) [Zh. Eksp. Teor. Fiz. **91**, 2008 (1986)].
[23] Jianwei Che *et al.*, J. Phys. Chem. **99**, 14 949 (1995).
[24] A. Saenz, J. Phys. B **33**, 4365 (2000).
[25] T. Zuo and A. D. Bandrauk, Phys. Rev. A **52**, R2511 (1995).
[26] T. Seideman, M. Y. Ivanov, and P. B. Corkum, Phys. Rev. Lett. **75**, 2819 (1995).
[27] H. Yu, T. Zuo, and A. D. Bandrauk, Phys. Rev. A **54**, 3290 (1996).
[28] E. Constant, H. Stapelfeldt, and P. B. Corkum, Phys. Rev. Lett. **76**, 4140 (1996).
[29] G. N. Gibson, M. Li, C. Guo, and J. Neira, Phys. Rev. Lett. **79**, 2022 (1997).
[30] D. Normand and M. Schmidt, Phys. Rev. A **53**, R1958 (1996).
[31] R. J. LeRoy, University of Waterloo, Level 7.4, A Computer Program for Solving the Radial Schrödinger Equation for Bound and Quasibound Levels.